State Estimation for Linearized MHD Flow

J. Chandrasekar, O. Barrero, A. Ridley, D. S. Bernstein, and B. De Moor

***Abstract*— A state estimation problem for linearized magnetohydrodynamic(MHD) flow is considered. The ideal MHD equations governing the flow of plasma in a three-dimensional channel are linearized about an equilibrium flow. Pseudospectral collocation methods are used to spatially discretize the linear partial differentiation equations and obtain a state-space model of the linearized dynamics. Three different discrete-time Kalman filtering algorithms are used to estimate the state variables, and their performance is analyzed.**

I. INTRODUCTION

Plasma, as a distinct state of matter, plays a crucial role in numerous branches of science and engineering. The Earth is constantly bombarded by low energy plasma emitted by the Sun. However, during flares and coronal mass ejections in the Sun, high energy plasma particles are ejected, causing problems with spacecraft and Earth-based systems [1, 2]. Furthermore, plasma is generated for low-thrust, but highly efficient electric propulsion systems for spacecraft [3]. Finally, plasma confinement and control is one of the main challenges of fusion-based power generation [4]. Plasma flow is the subject of magnetohydrodynamics (MHD), which involves both fluid dynamics and electrodynamics. Consequently, MHD is governed by coupled partial differential equations, which include both the Navier-Stokes equations and Maxwell's equations [5, 6].

The present paper is concerned with modeling and state estimation for uncontrolled plasma flows. Our ultimate goal is to apply state estimation techniques to space weather data in order to estimate the state of the plasma flow throughout a region. As a first step in this direction, we linearize the MHD equations for inviscid, incompressible flow in a 2-dimensional channel about a steady flow condition. To spatially discretize these equations, we consider both Fourier and Chebyshev pseudospectral collocation methods [7, 8].

Next, we analyze the stability of the truncated linear time-invariant model obtained by the Fourier collocation method. Stability tests show that the resulting model is Lyapunov stable. This test is thus inconclusive regarding the stability of the original nonlinear system. The spatially discretized model is then used as the basis for constructing state estimators. We consider the standard Kalman filter in recursive form along with numerically efficient variations, specifically, the reduced rank square root Kalman filter (RRSQRT-KF) and the singular square root Kalman filter (SSQRT-KF). The use of these filters is motivated by the fact that large-scale MHD models of the magnetosphere typically involve several million states [9].

This research was supported by the National Science Foundation Information Technology Research initiative, through Grant ATM-0325332.
J. Chandrasekar, D. S. Bernstein, and A. Ridley are with The University of Michigan, Ann Arbor, MI 48109-2140, (734) 764-3719, (734) 763-0578 (FAX), dsbaero@umich.edu
O. Barrero and B. De Moor are with Katholieke Universiteit Leuven, ESAT/SCD-SISTA Department, 3001 Heverlee (Leuven), Belgium, +32 (0) 16-321709, +32 (0) 16-321970 (FAX), obarrero@esat.kuleuven.ac.be, bart.demoor@esat.kuleuven.ac.be

II. IDEAL MHD EQUATIONS

TABLE I
LIST OF SYMBOLS

μ_0	permeability of free space (N A^2)
ϱ	average mass density of plasma (kg/m^3)
p	pressure (N/m^2)
γ	ratio of specific heats
$\vec{u}$	velocity of the fluid element (m/s)
$\vec{B}$	magnetic field (Tesla)

Magnetohydrodynamics (MHD) provides a macroscopic dynamical description of plasma in the presence of electromagnetic fields. We assume that the plasma flow occurs in a non-relativistic regime, and we neglect ionization and recombination, which alter the total number of plasma particles. Also, we assume that the conductivity of the plasma is infinite, that is, $\sigma = \infty$. The gravitational and Coriolis forces are also ignored. Under these simplifying assumptions the resulting ideal MHD equations are [2, 4, 5]

$$\frac{\partial \varrho}{\partial t} + \nabla \cdot (\varrho \vec{u}) = 0, \tag{2.1}$$

$$\frac{d}{dt}\left(\frac{p}{\varrho^{\gamma}}\right) = 0, \tag{2.2}$$

$$\varrho \frac{\partial \vec{u}}{\partial t} + \varrho\,(\vec{u}\cdot\nabla)\,\vec{u} = -\nabla p + \frac{1}{\mu_0}\left(\nabla \times \vec{B}\right) \times \vec{B}, \tag{2.3}$$

$$\nabla \times \left(\vec{u} \times \vec{B}\right) = \frac{\partial \vec{B}}{\partial t}, \tag{2.4}$$

$$\nabla \cdot \vec{B} = 0. \tag{2.5}$$

III. STEADY-STATE FLOW AND PERTURBATIONS IN A 2D CHANNEL

Next, we determine steady-state flow and magnetic field configurations that are consistent with the ideal

MHD equations. The domain in this case is the box $\Omega = \{(x,y) \in [L_{x_1}, L_{x_2}] \times [0, M]\}$. Consider a cold plasma (a plasma is cold when the pressure term is negligible in the momentum equation (2.3)), that is, $p \equiv 0$ in (2.3). Furthermore, we assume that the plasma flowing through a 2D channel as shown in Figure 1, is incompressible, which implies that the density is constant, temporally and spatially, that is, $\varrho = \varrho_0$ and hence the adiabatic equation of state (2.2) can be ignored. Let $\vec{u}_0$ and $\vec{B}_0$ be the steady state solution of the MHD equations (2.1)-(2.5), that is,

$$\frac{\partial \vec{u}_0}{\partial t} = 0, \quad \frac{\partial \vec{B}_0}{\partial t} = 0. \tag{3.1}$$

Hence, it follows from (3.1) and (2.1)-(2.5) that $\vec{u}_0$ and $\vec{B}_0$ satisfy

$$\nabla \cdot \vec{u}_0 = 0, \tag{3.2}$$

$$\varrho_0 (\vec{u}_0 \cdot \nabla) \vec{u}_0 = \frac{1}{\mu_0}(\nabla \times \vec{B}_0) \times \vec{B}_0, \tag{3.3}$$

$$\nabla \times \left(\vec{u}_0 \times \vec{B}_0\right) = 0, \tag{3.4}$$

$$\nabla \cdot \vec{B}_0 = 0. \tag{3.5}$$

Next, assume that the plasma flows along the $\hat{\mathbf{e}}_\mathbf{x}$ direction with a constant velocity so that $\vec{u}_0 = u_{0_x}\hat{\mathbf{e}}_\mathbf{x}$ and let the constant magnetic field be prescribed by $\vec{B}_0 = B_{0_y}\hat{\mathbf{e}}_\mathbf{y}$. Note that the prescribed velocity and magnetic field satisfy (3.2) and (3.5), respectively, and hence $\vec{u}_0 = u_{0_x}\hat{\mathbf{e}}_\mathbf{x}$ and $\vec{B}_0 = B_{0_y}\hat{\mathbf{e}}_\mathbf{y}$ are steady-state solutions of the ideal MHD equations.

Next, define the perturbation variables $\vec{u}_\delta$ and $\vec{B}_\delta$ by

$$\vec{u}_\delta \triangleq \vec{u} - \vec{u}_0, \quad \vec{B}_\delta \triangleq \vec{B} - \vec{B}_0. \tag{3.6}$$

Substituting $\varrho = \varrho_0$ and (3.6) into (2.1) yields

$$\frac{\partial \varrho_0}{\partial t} + \varrho_0 \nabla \cdot \vec{u}_0 + \varrho_0 \nabla \cdot \vec{u}_\delta = 0. \tag{3.7}$$

Since the density is constant, substituting (3.2) into (3.7) yields

$$\nabla \cdot \vec{u}_\delta = 0. \tag{3.8}$$

Substituting (3.6) into (2.3), and substituting (3.1) and (3.3) into the resulting equation, and ignoring second and higher order perturbation terms yields

$$\begin{aligned} &\varrho_0 \frac{\partial \vec{u}_\delta}{\partial t} + \varrho_0 (\vec{u}_0 \cdot \nabla)\vec{u}_\delta + \varrho_0 (\vec{u}_\delta \cdot \nabla)\vec{u}_0 \\ &\quad = \frac{1}{\mu_0}\left[\left(\left(\nabla \times \vec{B}_0\right) \times B_\delta\right) + \left(\left(\nabla \times \vec{B}_\delta\right) \times B_0\right)\right]. \end{aligned} \tag{3.9}$$

Substituting (3.6) into (2.4) yields

$$\nabla \times \left[(\vec{u}_0 + \vec{u}_\delta) \times \left(\vec{B}_0 + \vec{B}_\delta\right)\right] = \frac{\partial}{\partial t}\left(\vec{B}_0 + \vec{B}_\delta\right). \tag{3.10}$$

Substituting (3.1) and (3.4) into (3.10) and ignoring second order perturbation terms yields

$$\nabla \times \left(\vec{u_0} \times \vec{B_\delta}\right) + \nabla \times \left(\vec{u_\delta} \times \vec{B_0}\right) = \frac{\partial \vec{B}_\delta}{\partial t}. \tag{3.11}$$

Substituting (3.6) and (3.5) into (2.5) yields

$$\nabla \cdot \vec{B}_\delta = 0. \tag{3.12}$$

Hence, (3.9) yields

$$\frac{\partial \vec{u}_\delta}{\partial t} + c_1 \frac{\partial \vec{u}_\delta}{\partial x} = c_2 \frac{\partial \vec{B}_\delta}{\partial y} \tag{3.13}$$

and it follows from (3.11) that

$$\frac{\partial \vec{B}_\delta}{\partial t} + c_1 \frac{\partial \vec{B}_\delta}{\partial x} = c_3 \frac{\partial \vec{u}_\delta}{\partial y}, \tag{3.14}$$

where $c_1 \triangleq u_{0_x}$, $c_2 = B_{0_y}/(\varrho_0 \mu_0)$, and $c_3 \triangleq B_{0_y}$. Therefore, (3.8), (3.12), (3.13), and (3.14) are the linearized equations that govern the dynamics of the perturbation variables $\vec{u}_\delta$ and $\vec{B}_\delta$. Note that (3.13) and (3.14) resemble a two-dimensional wave equation.

Taking the partial derivative of (3.13) with respect to t and x yields

$$\partial_{tt}\vec{u}_\delta + c_1 \partial_{tx}\vec{u}_\delta = c_2 \partial_{ty}\vec{B}_\delta \tag{3.15}$$

and

$$\partial_{xt}\vec{u}_\delta + c_1 \partial_{xx}\vec{u}_\delta = c_2 \partial_{xy}\vec{B}_\delta, \tag{3.16}$$

respectively. Taking the partial derivative of (3.14) with respect to y yields

$$\partial_{yt}\vec{B}_\delta + c_1 \partial_{yx}\vec{B}_\delta = c_3 \partial_{yy}\vec{u}_\delta. \tag{3.17}$$

Dividing (3.15) by c_2, and multiplying (3.16) by $\frac{c_1}{c_2}$, and adding the resulting equation with (3.17) yields

$$\partial_{tt}\vec{u}_\delta = -2c_1 \partial_{tx}\vec{u}_\delta - c_1^2 \partial_{xx}\vec{u}_\delta + c_2 c_3 \partial_{yy}\vec{u}_\delta. \tag{3.18}$$

Note the symmetry in (3.13) and (3.14) with respect to $\vec{u}_\delta$ and $\vec{B}_\delta$. Hence, a similar procedure yields

$$\partial_{tt}\vec{B}_\delta = -2c_1 \partial_{tx}\vec{B}_\delta - c_1^2 \partial_{xx}\vec{B}_\delta + c_2 c_3 \partial_{yy}\vec{B}_\delta. \tag{3.19}$$

Now, the equations governing the perturbations in the velocity field $\vec{u}_\delta$ and the magnetic field $\vec{B}_\delta$, have been decoupled.

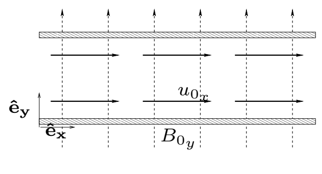

Fig. 1. The plasma is assumed to flow along the $\hat{\mathbf{e}}_\mathbf{x}$ direction only. The magnetic field is along $\hat{\mathbf{e}}_\mathbf{y}$ and is constant. The magnetic field exerts no pressure on the flow when the velocity of the plasma is parallel to the magnetic field. The pressure exerted by the magnetic field on the plasma when it flows perpendicular to the field depends on the gradient of the magnetic field, which is zero by assumption.

IV. State-Space Modeling using Spatial Discretization Methods

The partial differentiation equation (3.18) involves the ∂_{tx} operator and hence a separation of variable technique cannot be used to obtain an equivalent ordinary differential equation representation. Hence, we use spatial discretization methods to obtain an ODE model of the linearized perturbation dynamics. Let $\vec{u}_\delta = u_{\delta_x}\hat{\mathbf{e}}_\mathbf{x} + u_{\delta_x}\hat{\mathbf{e}}_\mathbf{y}$. It follows from (3.8) that there exists a scalar potential function $\psi(x, y, t)$ such that

$$u_{\delta_x} = \frac{\partial \psi}{\partial y}(x, y, t), \;\; u_{\delta_y} = -\frac{\partial \psi}{\partial x}(x, y, t). \tag{4.1}$$

Hence, it follows from (3.18) that

$$\partial_{tty}\psi + 2c_1\partial_{txy}\psi + c_1^2\partial_{xxy} = c_2c_3\partial_{yyy}\psi. \tag{4.2}$$

Assume $\psi(x, y, t)$ has a solution of the form

$$\psi(x, y, t) = U_m(x, t)W_m(y), \tag{4.3}$$

where for all $m = 0, 1, \ldots$, $U_m : \mathbb{R} \times \mathbb{R} \to \mathbb{R}$ and $W_m : \mathbb{R} \to \mathbb{R}$. Substituting (4.3) into (4.2) and dividing the resulting equation by $u_{\delta_x} = U_m(x, t)W'_m(y)$ yields

$$\frac{\partial_{tt}U_m(x,t)}{U_m(x,t)} + 2c_1\frac{\partial_{tx}U_m(x,t)}{U_m(x,t)} + c_1^2\frac{\partial_{xx}U_m(x,t)}{U_m(x,t)} = c_2c_3\frac{W'''_m(y)}{W'_m(y)}, \tag{4.4}$$

which implies that

$$\frac{W'''_m(y)}{W'_m(y)} = k_m, \tag{4.5}$$

where $k_m \in \mathbb{R}$ is a constant determined by the boundary conditions. We assume that the boundary conditions along $\hat{\mathbf{e}}_\mathbf{y}$ are periodic and given by

$$u_{\delta_x}(x, 0, t) = 0, \;\; u_{\delta_x}(x, M, t) = 0. \tag{4.6}$$

Note that (4.6) is a simplifying assumption and is not equivalent to the no-slip boundary conditions because viscosity has not been included in the ideal MHD equations. It follows from (4.1) that a solution to (4.5) that satisfies (4.6) is

$$W_m(y) = -w_{0,m}\cos\left(\frac{m\pi y}{M}\right), \tag{4.7}$$

where $w_{0,m}$ is determined by the initial condition, and can be assumed to be equal to unity without any loss of generality, and

$$k_m = -\omega_{\mathrm{n},m}^2 = -\left(\frac{m\pi}{M}\right)^2. \tag{4.8}$$

Hence, it follows from (4.4) that

$$\partial_{tt}U_m(x,t) + 2c_1\partial_{tx}U_m(x,t) + c_1^2\partial_{xx}U_m(x,t) + k_{0,m}U_m(x,t) = 0, \tag{4.9}$$

where $k_{0,m} \in \mathbb{R}$ is defined by $k_{0,m} \triangleq c_2c_3\omega_{\mathrm{n},m}^2 > 0$.

A. Fourier Collocation Method

In this section, we assume that the boundary conditions are periodic along the $\hat{\mathbf{e}}_\mathbf{x}$ direction, and hence, express $U_m(x, t)$ as a Fourier series in x with time-varying coefficients. Let $L_{x_1} = 0$ and $L_{x_2} = 2\pi$, and, for $i = 1, \ldots, n$, let $x_{\mathrm{f}i} \triangleq \frac{2\pi(i-1)}{n}$, be the n collocation points along the $\hat{\mathbf{e}}_\mathbf{x}$ direction. Define $q_m^{x_{\mathrm{f}i}}$ by

$$q_m^{x_{\mathrm{f}i}} \triangleq U_m(x_{\mathrm{f}i}, t). \tag{4.10}$$

Next, for all $k = -\frac{n}{2}, \ldots, \frac{n}{2}-1$, define the discrete Fourier coefficients $\tilde{q}_{m_k}$ by $\tilde{q}_{m_k} \triangleq \frac{1}{n}\sum_{i=1}^{n} q_m^{x_{\mathrm{f}i}} e^{-\jmath(kx_{\mathrm{f}i})}$ so that $U_m(x, t)$ can be expressed by the discrete Fourier series

$$U_m(x,t) = \sum_{k=-\frac{n}{2}}^{\frac{n}{2}-1} \tilde{q}_{m_k} e^{\jmath(kx)}. \tag{4.11}$$

Next, define $Q_m \in \mathbb{R}^n$ by

$$Q_m \triangleq \left[\begin{array}{ccc} q_m^{x_{\mathrm{f}1}} & \cdots & q_m^{x_{\mathrm{f}n}} \end{array}\right]^{\mathrm{T}}. \tag{4.12}$$

Using the Fourier collocation differentiation matrix [8] in (4.8) yields

$$\ddot{Q}_m + 2c_1\mathcal{D}_{\mathrm{F}n}\dot{Q}_m + c_1^2\mathcal{D}_{\mathrm{F}n}^2 Q_m + k_{0,m}Q_m = 0, \tag{4.13}$$

where $\mathcal{D}_{\mathrm{F}n} \in \mathbb{R}^{n\times n}$ and the (i, j)th element of $\mathcal{D}_{\mathrm{F}n}$ is given by

$$\mathcal{D}_{\mathrm{F}n_{(i,j)}} = \begin{cases} \frac{1}{2}(-1)^{i+j}\cot\left[\frac{(i-j)\pi}{n}\right], & i \neq j, \\ 0, & i = j. \end{cases} \tag{4.14}$$

A state-space representation of (4.13) is

$$\left[\begin{array}{c} \dot{Q}_m \\ \ddot{Q}_m \end{array}\right] = A_m \left[\begin{array}{c} Q_m \\ \dot{Q}_m \end{array}\right], \tag{4.15}$$

where $A_m \in \mathbb{R}^{2n\times 2n}$ is defined by

$$A_m \triangleq \left[\begin{array}{cc} 0_n & I_n \\ -(c_1^2\mathcal{D}_{\mathrm{F}n}^2 + k_{0,m}I_n) & -2c_1\mathcal{D}_{\mathrm{F}n} \end{array}\right]. \tag{4.16}$$

Note that A_m can be factored as

$$A_m = P\left[\begin{array}{cc} -c_1\mathcal{D}_{\mathrm{F}n} + \jmath k_{0,m}^{1/2}I_n & 0 \\ S & -c_1\mathcal{D}_{\mathrm{F}n} - \jmath k_{0,m}^{1/2}I_n \end{array}\right]P^{-1}, \tag{4.17}$$

where $S \in \mathbb{R}^{n\times n}$ is defined by $S \triangleq -\left(c_1^2\mathcal{D}_{\mathrm{F}n}^2 + k_{0,m}I_n\right)$, $T \in \mathbb{C}^{n\times n}$ is defined by $T \triangleq \left(c_1\mathcal{D}_{\mathrm{F}n} - \jmath k_{0,m}^{1/2}I_n\right)S^{-1}$, and $P \in \mathbb{R}^{2n\times 2n}$ is defined by

$$P \triangleq \left[\begin{array}{cc} I_n & T \\ 0_n & I_n \end{array}\right], \tag{4.18}$$

which implies that

$$\mathrm{spec}(A_m) = \mathrm{spec}(-c_1\mathcal{D}_{\mathrm{F}n} + \jmath k_{0,m}^{1/2}I_n) \cup \mathrm{spec}(-c_1\mathcal{D}_{\mathrm{F}n} - \jmath k_{0,m}^{1/2}I_n). \tag{4.19}$$

It follows from (4.14) that $\mathcal{D}_{\mathrm{F}n}$ is skew symmetric and hence all its eigenvalues lie on the imaginary axis. Hence, (4.19) implies that the eigenvalues of A_m are also confined to the imaginary axis, that is, for all $\lambda \in \mathrm{spec}(A_m)$, $\mathrm{Re}(\lambda) = 0$. Note that (4.13) is a second order system and can be expressed as

$$M\ddot{Q}_m + G\dot{Q}_m + KQ_m = 0, \tag{4.20}$$

where $M = I_n$, $G = 2c_1\mathcal{D}_{\mathrm{F}n}$, and $K = c_1^2\mathcal{D}_{\mathrm{F}n}^2 + k_0I_n$. Since $GK = KG$ and $K + \frac{1}{4}GG^{\mathrm{T}}$ is positive definite, it follows from Proposition 3 of [10] that (4.13) is Lyapunov stable.

Note that (4.13) represents the dynamics of the mth mode and it follows from the principle of superposition that the solution to (4.2) is given by $\psi(x, y, t) = \sum_{m=1}^{\infty} U_m(x, t)W_m(y)$. Retaining r modes and defining the modal state vector $\tilde{Q} \in \mathbb{R}^{2nr}$ by $\tilde{Q} \triangleq \left[\begin{array}{ccccc} Q_1^{\mathrm{T}} & \dot{Q}_1^{\mathrm{T}} & \cdots & Q_r^{\mathrm{T}} & \dot{Q}_r^{\mathrm{T}} \end{array}\right]^{\mathrm{T}}$, it follows from (4.15) and (4.16) that

$$\dot{\tilde{Q}} = A\tilde{Q}, \tag{4.21}$$

where $A \in \mathbb{R}^{2nr\times 2nr}$ is the block-diagonal matrix

$$A \triangleq \begin{bmatrix} A_1 & 0 & \cdots \\ 0 & \ddots & 0 \\ \vdots & 0 & A_r \end{bmatrix}. \tag{4.22}$$

Hence, $\mathrm{spec}(A) = \mathrm{spec}(A_1) \cup \cdots \cup \mathrm{spec}(A_r)$ and, for all $\lambda \in \mathrm{spec}(A)$, $\mathrm{Re}(\lambda) = 0$.

Let $y_{\mathrm{x_{out}},i,j} \triangleq u_{\delta_x}(x_{\mathrm{f}_i}, y_j, t)$ be the measured perturbation in the flow velocity u_x from u_{0_x} at $(x_{\mathrm{f}i}, y_j)$, where $x_{\mathrm{f}i}$ is one of the grid points. It follows from (4.1), (4.3), and (4.10) that

$$y_{\mathrm{x_{out}},i,j} = \partial_y \psi(x,y,t)\Big|_{(x=x_{\mathrm{f}_i}, y=y_j)} = C_{\mathrm{x}_{i,j}}\tilde{Q}, \tag{4.23}$$

where $C_{\mathrm{x}_{i,j}} \in \mathbb{R}^{1\times 2nr}$ has entries $C_{\mathrm{x}_{i,j}} = \begin{bmatrix} C^1_{\mathrm{x}_{i,j}} & \cdots & C^m_{\mathrm{x}_{i,j}} \end{bmatrix}$, and, for all $m = 1,\ldots,r$, $C^m_{\mathrm{x}_{i,j}} \in \mathbb{R}^{2n}$ is defined by

$$C^m_{\mathrm{x}_{i,j}} \triangleq \begin{bmatrix} 0_{i-1} & W'_m(y_j) & 0_{2n-i} \end{bmatrix}. \tag{4.24}$$

Next, we consider the case when the measurement $\tilde{y}_{\mathrm{y_{out}},i,j} \triangleq u_{\delta_y}(x_{\mathrm{f}i}, y_j, t)$ is the perturbation in the flow velocity u_y from u_{0_y} at (x_{f_i}, y_j). It follows from (4.1) that

$$\tilde{y}_{\mathrm{y_{out}},i,j} = -\partial_x \psi(x,y,t)\Big|_{(x=x_{\mathrm{f}_i}, y=y_j)}. \tag{4.25}$$

Using (4.3), (4.10), and the Fourier collocation differentiation matrix D_{F_n} in (4.25) yields

$$\tilde{y}_{\mathrm{y_{out}},i,j} = -C_{\mathrm{y}_{i,j}} D_{\mathrm{F}_n}\tilde{Q}, \tag{4.26}$$

where $C_{\mathrm{y}_{i,j}} \in \mathbb{R}^{1\times 2nr}$ has entries $C_{\mathrm{y}_{i,j}} = \begin{bmatrix} C^1_{\mathrm{y}_{i,j}} & \cdots & C^m_{\mathrm{y}_{i,j}} \end{bmatrix}$, and, for all $m = 1,\ldots,r$, $C^m_{\mathrm{y}_{i,j}} \in \mathbb{R}^{2n}$ is defined by

$$C^m_{\mathrm{y}_{i,j}} \triangleq \begin{bmatrix} 0_{i-1} & W_m(y_j) & 0_{2n-i} \end{bmatrix}. \tag{4.27}$$

Note that (3.18) and (3.19) are similar and hence the solution to $\vec{B}_\delta$ is similar to that of $\vec{u}_\delta$, and the constants are determined by the initial and boundary values of the magnetic field instead of the velocity field.

B. Chebyshev Collocation Method

Next, we express $U_m(x,t)$ as a Chebyshev series in x with time varying coefficients. Let $L_1 = -1$ and $L_2 = 1$, and, for all $i = 1,\ldots,n$, let $x_{ci} = -\cos\left[\frac{(i-1)\pi}{n-1}\right]$ be the n Gauss-Lobatto grid points in the interval $[-1,1]$ (see [7, 8]). Consider a solution of the form (4.3) and define $q_m^{x_{ci}} \triangleq U_m(x_{ci}, t)$. The truncated Chebyshev series expansion for the solution $U_m(x,t)$ is (see [7])

$$U_m(x,t) = \sum_{k=0}^{n-1} \tilde{q}_{m_k}\phi_k(x), \tag{4.28}$$

where $\phi_k(x) \triangleq \cos(k\cos^{-1}(x))$, and, for all $k = 0,\ldots,n-1$, $\tilde{q}_{m_k}$ is defined by

$$\tilde{q}_{m_k} \triangleq \frac{1}{\gamma_k}\sum_{i=1}^{n} q_m^{x_{ci}}\phi_k(x_i)w_i, \tag{4.29}$$

where

$$\gamma_k = \begin{cases} \pi, & k=0 \text{ or } k=n-1, \\ \frac{\pi}{2}, & 0<k<n-1, \end{cases} \quad w_i = \begin{cases} \frac{\pi}{2(n-1)}, & i=1 \text{ or } i=n, \\ \frac{\pi}{n-1}, & 1<i<n. \end{cases} \tag{4.30}$$

Next, defining $Q_m \in \mathbb{R}^n$ by (4.12) with $q_m^{x_{\mathrm{f}i}}$ replaced by $q_m^{x_{ci}}$ and using the Chebyshev collocation differentiation matrix (see [8]) in (4.8) yields (4.13) with $\mathcal{D}_{\mathrm{F}n}$ replaced by $\mathcal{D}_{\mathrm{C}n}$, where the (i,j)th entry of $\mathcal{D}_{\mathrm{C}n}$ is defined by

$$\mathcal{D}_{\mathrm{C}n_{(i,j)}} = \begin{cases} \frac{c_i}{c_j}\frac{(-1)^{i+j}}{(x_{ci}-x_{ci})}, & i \neq j, \\ \frac{-x_{ci}}{2(1-x^2_{ci})}, & 1 < i = j \leq n, \\ \frac{2(n-1)^2+1}{6}, & i=j=1, \\ -\frac{2(n-1)^2+1}{6}, & i=j=n, \end{cases} \tag{4.31}$$

and c_i is defined by

$$c_i = \begin{cases} 2, & i=1 \text{ or } i=n, \\ 1, & 1<i<n. \end{cases} \tag{4.32}$$

The state-space model is then given by (4.21), where A_m is defined by (4.16) with $\mathcal{D}_{\mathrm{F}n}$ replaced by $\mathcal{D}_{\mathrm{C}n}$. The outputs $y_{\mathrm{x_{out}},i,j} \triangleq u_{\delta_x}(x_{ci}, y_j, t)$ and $y_{\mathrm{y_{out}},i,j} \triangleq u_{\delta_y}(x_{ci}, y_j, t)$ are given by (4.23)-(4.24).

In both cases, namely, the Fourier collocation and mapped Chebyshev collocation, all the eigenvalues of A are confined to the imaginary axis. Due to the roundoff errors in the mapped Chebyshev collocation method, the absolute value of the eigenvalues is very large, which implies that the dynamics as given in (4.21) is oscillatory with very high frequency. Hence, the Fourier collocation method was chosen for simulating the MHD flow. Furthermore, the perturbation u_{δ_x} at various collocation points is the plant output in all the simulations.

V. Kalman Filtering Estimator

In this section, three state space observers, namely, the standard Kalman filter (KF) [13], the reduced rank square root Kalman filter (RRSQRT-KF) [14], and the singular square root Kalman filter (SSQRT-KF) [15], are used to estimate the outputs of the linearized MHD flow system under different measurement noise conditions.

Consider the following state space representation for the linearized MHD system

$$x_{k+1} = Ax_k + w_k \tag{5.1}$$

$$y_k = Cx_k + v_k, \tag{5.2}$$

where $x_{k+1} = \tilde{Q}_{k+1}$, $C = C_{x_{i,j}}$, $y_k = y_{x_{out_{i,j}}}$, $w_k \in \mathbb{R}^{2nr}$ is the process noise, and $v_k \in \mathbb{R}^p$ the measurement noise. Furthermore, assume that w_k and v_k are uncorrelated white Gaussian noise processes with zero mean and covariance matrices Q and R, respectively.

A. Discrete Time Kalman Filter

Consider the discrete-time dynamical system described by (5.1) and (5.2). For this system, we take a state estimator of the form

$$\hat{x}_{k|k} = \hat{x}_{k|k-1} + L_k(y_k - \hat{y}_{k|k-1}), \quad k \geq 0, \tag{5.3}$$

where $L_k \in \mathbb{R}^{n\times m}$ and $\hat{x}_{k|k}$ is the estimate of x_k based on observations up to time k, with output

$$\hat{y}_{k|k-1} = C\hat{x}_{k|k-1}. \tag{5.4}$$

Kalman [16] found a recursive solution to obtain the optimal L_k which minimizes the error estimation error defined by

$$e_{k|k} = x_k - \hat{x}_{k|k}. \tag{5.5}$$

The solution can be summarized as follows:
Define the error covariance matrix

$$P_{k|k} \triangleq E[e_{k|k}e_{k|k}^T] \tag{5.6}$$

where $E[\cdot]$ denotes expectation.

1) Compute the prior error covariance matrix and the estimated states
$$P_{k|k-1} = A_{k-1}P_{k-1|k-1}A_{k-1}^{\mathrm{T}} + Q_{k-1}. \tag{5.7}$$
$$\hat{x}_{k|k-1} = A_{k-1}\hat{x}_{k-1|k-1} \tag{5.8}$$
2) Compute the Kalman gain
$$L_k = P_{k|k-1}C_k^T(R_k + C_kP_{k|k-1}C_k^T)^{-1}, \tag{5.9}$$
3) Update the estimated states using (5.3) and (5.4)
4) Update the error covariance matrix
$$P_{k|k} = (I_n - L_kC_k)P_{k|k-1}. \tag{5.10}$$

B. SSQRT-KF Algorithm

SSQRT-KF is based on the fact that the process noise is negligible or zero, therefore we can assume $Q = 0$. By definition, the Schur complement of (5.10) with $Q = 0$ is the matrix,

$$M = \begin{pmatrix} R + CP_{k|k-1}C^T & CP_{k|k-1} \\ P_{k|k-1}C^T & P_{k|k-1} \end{pmatrix}, \tag{5.11}$$

with

$$R \triangleq L_RL_R^T, \quad P_{k|k-1} \triangleq S_{k|k-1}S_{k|k-1}^T. \tag{5.12}$$

A QR decomposition of M yields

$$\begin{pmatrix} L_R & CS_{k|k-1} \\ 0 & S_{k|k-1} \end{pmatrix} U_k = \begin{pmatrix} \hat{F}_k & 0 \\ \hat{K}_k & S_{k|k} \end{pmatrix}, \tag{5.13}$$

where U_k is orthogonal and $S_{k|k}$ is $n \times l$, with l chosen larger than the number of unstable eigenvalues of A, and $P_{k|k} = S_{k|k}S_{k|k}^T$. Note that the QR decomposition is computed for a small matrix of size $(p + l) \times p$ making it cheap to compute. On the other hand, the Kalman filter gain can be computed from $\hat{F}_k$ and $\hat{K}_k$ as

$$L_k = \hat{K}_k\hat{F}_k^{-1}, \tag{5.14}$$

provided that F_k is invertible. If the measurements are uncorrelated, i.e., R diagonal, then F_k will be diagonally dominant, therefore instead of computing F_k^{-1}, we invert its diagonal entries to obtain a diagonal approximation of F_k^{-1}. Moreover, if A and C are sparse, the construction of the left factor in the left hand side of (5.13) is cheap as well.

A key characteristic of SSQRT-KF algorithm is that the spectrum of the state space observer dynamics matrix $A - L_kC$ is constructed by reflecting the eigenvalues of A with $|\lambda| > 1$ to their unit circle mirror images $1/|\lambda|$, and leaving the eigenvalues with $|\lambda| < 1$ unchanged.

C. RRSQRT-KF Algorithm

In the RRSQRT-KF estimator the square root factors are based on an eigendecomposition. Let $P_{k|k-1} = V_k\Lambda_kV_k^T$ be the eigendecomposition of the error covariance matrix $P_{k|k-1}$, so that $S_{k|k-1} = V_k\Lambda_k^{1/2}$ is a square root factor of $P_{k|k-1}$. The error covariance matrix is now approximated by using only q leading eigenvalues. With the ordering $|\lambda_1| \geq \ldots \geq |\lambda_n| \geq 0$, an approximation is obtained by truncating $S_{k|k-1}$ after the first q columns. The algorithm is as follows:

1. Update $\hat{x}_{k|k-1} = A_{k-1}\hat{x}_{k-1|k-1} + B_{k-1}u_{k-1}$
2. Update $S_{k|k-1} = [A_{k-1}S_{k-1|k-1}\ L_{Q_{k-1}}]$
3. Rank reduction of the error covariance:
$$S^*_{k|k-1} = [S_{k|k-1}\ V_k]_{1:n,1:q},$$
where $S_{k|k-1}^TS_{k|k-1} = V_k\Lambda_kV_k^T$
4. Compute L_k and $S_{k|k}$ using the scalar update of Potter [14] for independent measurements as follows,
$S_{k|k} = S^*_{k|k-1}$,
for $i = 1$ to p,
$$\begin{aligned} H &= S^{*T}_{k|k-1}C_k(i,:)^T \\ F &= (H^TH + R_k(i,i))^{-1} \\ L_k(:,i) &= S^*_{k|k-1}HF \\ S_{k|k} &= S_{k|k} - L_kH^T(1 + (FR_k(i,i))^{1/2})^{-1}. \end{aligned}$$
end
5. Compute $\hat{x}_{k|k} = \hat{x}_{k|k-1} + L_k(y_k - C_k\hat{x}_{k|k-1})$

If the measurements are correlated see details in [14].

VI. State Estimation for the Linearized MHD Model

We consider a 20×20 grid with equidistant points (the grid points along the $\hat{\mathbf{e}}_{\mathbf{x}}$ direction are the Fourier collocation points), where $0 < x < 2\pi$, $0 < y < 1$, and sample time $T_s = 10^{-3}$ seconds. The number of modes retained is $m = 5$ and hence, $A_{\mathrm{d}} \in \mathbb{R}^{200\times200}$, and $C_{\mathrm{d}} \in \mathbb{R}^{400\times200}$. Although the system may be fully observable with just one measurement output, the discrete-time linearized system turns out to be marginally observable, because all the poles are clustered on the unit circle, which entails numerical round-off error. Figure 2 shows that at least 10 output measurements are needed to guarantee the full observability of the system. Hence, we use 50 measurements to ensure that the system is observable. It

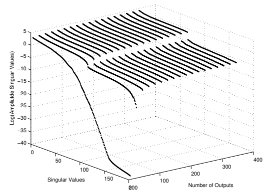

Fig. 2. Logarithm of the singular values of the observability matrix for different number of measurements. We observe that the condition number of the observability matrix is high for a small number of measurements and the condition number is small when the number of measurements is larger than ~ 10 .

can be seen in Figure 4 that all the three methods converge very slowly, this is due to the fact that the system is marginally observable as can be seen in Figure 3.

The classical KF has a better performance compare to the others, because the matrix dynamics of the error (Figure 3 top-right) is stable, while the matrices error dynamics of the other filters are not. This happen because the KF gain approximation made for the suboptimal techniques are based on using the most important modes, something no possible for this case, because all the modes are equally important. As a result the suboptimal KF estimators will be oscillatory as can be seen in Figure 4.

VII. Conclusion

A discrete-time linearized model for the flow of plasma in a two-dimensional channel was obtained. The obtained model is marginally stable and has oscillatory dynamics which makes the system difficult to observe. Three different state space observers were studied, namely, Kalman filter, RRSQRT-KF filter, and SSQRT-KF filter.

Although the Kalman filter performs well, and is very reliable and robust as shown in Figure 4, it

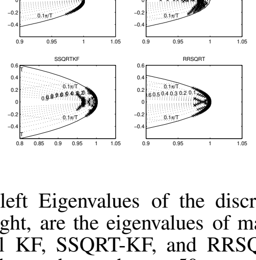

Fig. 3. In the top-left Eigenvalues of the discrete model, top-right, bottom-left, bottom-right, are the eigenvalues of matrix dynamics of the error for the classical KF, SSQRT-KF, and RRSQRT-KF, respectively. For the three methods we have chosen 50 output measurements. For RRSQRT-KF $q = 50$, and for SSQRT-KF $l = 50$.

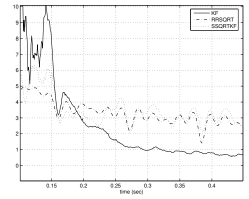

Fig. 4. RMSE of the estimated outputs taking 50 measurements. Solid line KF, dash-dotted line SSQRT-KF, and dotted line RRSQRT-KF. The $\mathrm{SNR} = 13\mathrm{dB}$ for the measurement noise.

converges slowly. Another drawback of the Kalman filter is that it is prohibitive to compute for large scale systems. On the other hand, RRSQRT-KF and SSQRT-KF exhibit numerical problems due to the fact that the system is marginally observable which makes it difficult to find a stable suboptimal KF.

Moreover, these methods are based on the square root algorithm, and hence their convergence rate is low when the eigenvalues of A_d are located very close to the unit circle (see Figure 3). Therefore, we cannot exploit the advantages of the proposed suboptimal Kalman filters for the linearized MHD model.

References

[1] I. A. Daglis, *Space Storms and Space Weather Hazards*, Kluwer Academic Publishers, 2001.

[2] M. B. Kallenrode, *Space Physics*, Springer, 2000.

[3] P. Y. Peterson, A. D. Gallimore, and J. M. Haas, "An experimental investigation of the internal magnetic field topography of an operating Hall thruster," *Physics of Plasmas*, vol. 9, pp. 4354-4362, 2002.

[4] J. P. Freidberg, *Ideal Magnetohydrodynamics*, Plenum Press, 1987.

[5] Tamas. I. Gombosi, *Physics of the Space Environment*, Cambridge University Press, 1998.

[6] P. C. Kendall and C. Plumpton, *Magnetohydrodynamics with hydrodynamics*, Pergamon Press, 1964.

[7] O. M. Aamo and M. Kristic, *Flow Control by Feedback - Stabilization and Mixing*, Springer, 2003.

[8] C. Canuto, M. Y. Hussaini, A. Quarteroni, and T. A. Zang, *Spectral Methods in Fluid Dynamics*, Springer-Verlag, 1988.

[9] C. P. T. Groth, D. L. D. Zeeuw, T. I. Gombosi, and K. G. Powell, "Global three-dimensional MHD simulation of a space weather event: CME formation, interplanetary propagation, and interaction with the magnetosphere," *J. Geo. Phy. Res.*, vol. 105, pp. 25,053-25,078, 2000.

[10] D. S. Bernstein and S. P. Bhat, "Lyapunov Stability, Semistability and Asymptotic Stability of Matrix Second Order Systems," *Trans. of ASME.*, 50th Anniversary Design Issue, pp. 145-153, 1995.

[11] W. S. Don and A. Solomonoff, "Accuracy Enhancement for Higher Derivatives using Chebyshev Collocation and a Mapping Technique," *SIAM J. Sci. Comp.*, vol. 18, pp. 1040-1055, 1997.

[12] M. Morf and T. Kailath, "Square-Root Algorithms for Least-Squares Estimation," *IEEE Trans. Auto. Contr*, vol. 20, pp. 487-497, 1975.

[13] R. E. Kalman, "A New Approach to Linear Filter and Prediction Theory," *J. Basic. Engr.*, vol. 82D, pp. 35-45, 1960.

[14] M. Verlaan and A. W. Heemink, "Reduced Rank Square Root Filters for Large Scale Data Assimilation Problems," *2nd Int. Symp. on Assimilation of Obs. in Met. & Ocea, WMO*, pp. 247-252, 1995.

[15] O. Barrero and B. De Moor, "A Singular Square Root Algorithm for Large Scale Systems," *Proc. 15th IASTED Int. Conf. Model. Sim., Marina del Rey, USA*, March 2004.

[16] R. Kalman and R. Bucy, "New Results in Linear Filtering and Prediction Theory," *J. Basic. Engr*, vol. 83D, pp. 95-108, 1961.